Electrodeposition of a protective Cu/Ni-P deposit on AZ91D magnesium alloy

ZHANG Shan, CAO Fahe, ZHENG Junjun, ZHANG Zhao, ZHANG Jianqing
(Department of Chemistry, Zhejiang University, HangZhou 310027)

Abstract: High corrosion resistance Cu/Ni-P coatings were electrodeposited on AZ91D magnesium alloy via suitable pretreatments, such as one-step acid pickling-activation, once zinc immersion and environment-friendly electroplated copper as the protective under-layer, which made Ni-P deposit on AZ91D Mg alloy in acid plating baths successfully. The pH value and current density of the Ni-P solution were optimized to obtain high corrosion resistance Ni-P coatings. With increasing the phosphorous content of the Ni-P coatings, the deposits were found to gradually transform to amorphous structure and the corrosion resistance increased synchronously. The anticorrosion ability of AZ91D Mg alloy was greatly improved by the amorphous Cu/Ni-P deposits, which was investigated by potentiodynamic polarization curve and electrochemical impedance spectroscopy (EIS). The corrosion current density (Icorr) of the coated Mg alloy substrate is about two orders of magnitude less than that of the uncoated.

Keywords:AZ91D Mg alloy; Electrodeposition; Ni-P; Corrosion Resistance

0 Introduction

The high strength–to–weight ratio makes magnesium alloy very desirable in many industries. However, their high chemical reactivity and poor corrosion resistance have limited their widespread applications [1]. Therefore, it is necessary to make a protective surface before their applications.

Several surface coating treatments have been proposed to meet the requirements of corrosion protective for Mg alloy, such as metal coatings [2-4], conversion coatings [5], anodization [6], micro-arc oxidation treatment [7], organic coatings [8] and vapor-phase processes [9]. Compared with these surface coating treatments, electrodeposition technique has been proved to be less energy consumption, lower cost and easier to control. Ordinary coatings, such as nickel, copper and zinc coating electrodeposited on Mg alloy were very well documented in the literatures [3, 4, 10-12], can only provide the under-layer for further metal plated and a physical barrier to corrosion attack of magnesium substrate. So, any coatings on magnesium alloys should be as uniform and pore-free as possible.

P-containing alloy coatings obtained by electrodeposition have been widely used to prevent corrosion. Ni-P coatings have proved to be high corrosion resistance owning to their special amorphous, microcrystal or nanocrystalline structure changing with various phosphorus contents [13]. A. Bai [14] and I. V. Petukhov [15] reported that the corrosion potential of Ni-P deposits in brine media was nobler than that of Ni deposit and the corrosion current of Ni-P deposits was less. Therefore, the application range of magnesium alloy can be widely enlarged by electrodepositing Ni-P coatings. Generally, there are two main difficulties in electrodeposition on magnesium alloy. One is that the chemical reactivity of Mg alloy which is unstable below pH of 10.0 is extremely high; the other is that there are heterogeneous phases with different standard electrode potentials in Mg alloy and then galvanic corrosion will destructively affect the work electrode be electroplated in solution media [16]. Meanwhile, phosphorus co-deposition with nickel are usually

Foundations: Doctoral Fund of Ministry of Education of China (Grant No. 200803351092) and National Natural Science Foundation of China (No. 50801056).
Correspondance author: CAO Fahe, (1979-), Male, Associate Professor, Corrosion Electrochemistry. E-mail: nelson_cao@zju.edu.cn
Brief author introduction:ZHANG Shan, (1987-), Female, Graduate Student, Corrosion and Protection of Magnesium alloy

in low pH value electrolyte [17, 18] in which Mg alloy is prone to corrosive dissolution. Therefore, the pretreatment with an aim to make a protective layer for Mg Alloy is an essential part before Ni-P coatings being electrodeposited. The chromium trioxide and poisonous cyanide used in conventional pretreatment process (degrease→ acid pickling→ acid activation → zinc immersion → copper cyanide electroplating) [16] are acutely toxic to human and contaminative to environment. Electrochemical behaviors of the magnesium alloy substrates in various pretreatment solutions were studied by G. Yu et al. [19], the pretreatments processes, $K_4P_2O_7$ activation after HNO_3+H_3PO_4 pickling and one-step $KMnO_4$ pickling-activation for AZ91D Mg alloy, were suggested for Ni and Cu electroplating, respectively. A pretreatment with galvanostatic etching before copper electrodeposition on Mg alloy was developed by Neubert and Huang et al. [4, 10, 11]. The results indicate the copper electrodeposition is an effective pretreatment of magnesium alloy. In our previous study, Zhao et al. [12] investigated the effect of zinc immersion pretreatment on the electrodepositing of Ni on AZ91D magnesium alloy and twice zinc immersion which is complex was used in the pretreatment process. All these studies above are about electrodepositing physical protective Ni or Cu coating and electroless Ni-P coatings on Mg alloy.

To date, no literatures have been reported about electrodepositing Ni-P coatings on Mg alloy. The crucial pretreatment and suitable electrodeposition technology for Ni-P coatings is thought to be the key points. In the present work, suitable pretreatments, such as one-step HF acid pickling-activation, once zinc immersion and environment-friendly plated copper as under-layer, were applied in order to electro-deposit high corrosion resistance Ni-P coatings on AZ91D magnesium alloy successfully. Furthermore, the effect of solution pH value, current density on the phosphorus content and corrosion resistance of Ni-P deposits was also investigated.

1 Experimental procedure

Die-cast AZ91D magnesium alloy composed of 91.0% Mg, 8.77% Al, 0.74% Zn and other elements (in mass fraction) was used as the testing material. Prior to experiment, the testing specimens were cut into cylinder pieces (Φ8 mm) covering with polytetrafluoroethylene (PTFE). A Cu bar was used to provide electric connection to the specimens. The surface of each specimen was gradually polished with silicon carbide papers up to 1000 grade, followed by polishing with 2.5 μm diamond spray, rinsed with distilled water, then washed with acetone and dried in cool air. The test electrolyte was neutral 3.5 wt. % NaCl solutions. All of the solutions were prepared with analytical-purity reagents and distilled water.

The process flow, the main parameters for pretreatment and electrodeposition of Ni-P coatings on AZ91D Mg alloy were listed in Table 1.

Table 1 The process flow and the parameters for pretreatment of AZ91D Mg alloy and electrodeposition of Ni-P coatings on AZ91D Mg alloy (RT=room temperature).

Process	Solution compositions		Conditions
1 Acetone cleaning	Acetone		1-3 min RT
2 Pickling -activation	HF (40%)	54 ml/L	30 s RT
3 Zinc immersion	$ZnSO_4·7H_2O$ $K_4P_2O_7$ Na_2CO_3	30 g/L 180 g/L 5 g/L	3.5-5 min 70 ℃ pH =10.0 ± 0.2
4 Copper plating	$Cu_2P_2O_7$ $K_4P_2O_7$ $(NH_4)_3C_6H_5O_7$	28 g/L 100-150 g/L 60-70 g/L	12 min 40 ℃ pH= 8.2-8.8 D_k=1.20 A/dm^2
5 Electrodeposition Ni-P	$NiSO_4·6H_2O$ $NiCl_2·6H_2O$ H_3PO_3 H_3PO_4 Additives	200 g/L 45 g/L 40 g/L 30 g/L	20 min pH=0.84-2.20 70℃ D_k=1.0-10.0 A/dm^2 r=900 r/min

A transistor constant potential/current device (Model ZF-9, China) was used to provide dc current during Cu and Ni-P electroplating. Potentiodynamic polarization measurements were performed on CHI660A electrochemical workstation (Shanghai Chenhua Instruments Company, China) at a scan rate of 0.5 mV/s from -250 mV to 250 mV vs. open circuit potential (OCP). The electrochemical impedance spectroscopy (EIS) measurements were conducted at the OCP. The employed amplitude of the sinusoidal signal was 10 mV peak to peak and the frequency range studied was from 100 KHz to 10 mHz. A saturated calomel electrode (SCE) as reference electrode (separated by a salt bridge from the cell solution), a large platinum sheet as auxiliary electrode and the specimen of exposed area of 0.5027 cm^2 as working electrode were used in a traditional three-electrode system in electrochemical measurements.

The surface morphology and composition were characterized by SEM and EDX using a SIRION (FEI Co., Holland). The structure of AZ91 substrate after different steps of pretreatment and Ni-P deposit was examined by XRD with Cu Kα radiation using a XPERT-PRO (PANalytical B.V, Holland).

2 Results and discussion

2.1 Pretreatment of AZ91D Mg alloy

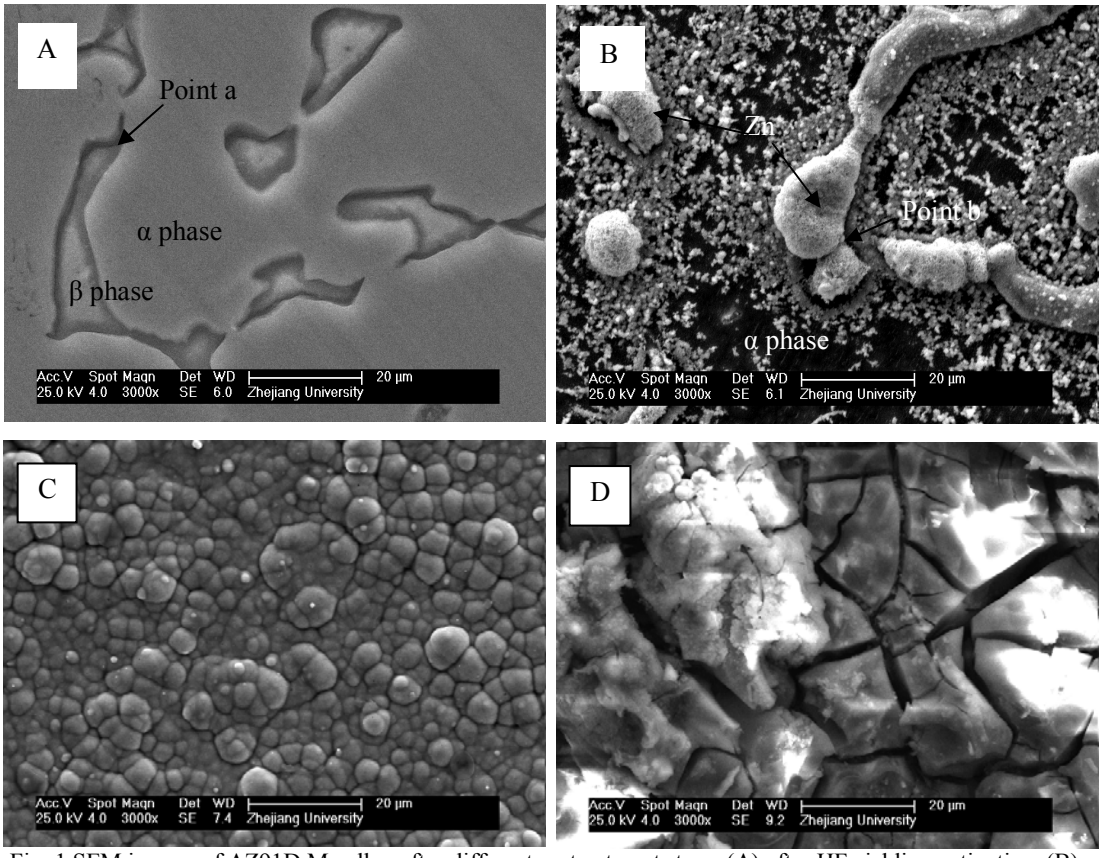

Fig. 1 SEM images of AZ91D Mg alloy after different pretreatment steps: (A) after HF pickling-activation, (B) after Zn immersion, (C) after copper plating, (D) Ni-P coated without Cu plated as under-layer.

Fig. 1 shows the SEM images of the specimen surface after different process. EDX results for element composition (wt%, mass fraction) of specimen surface are listed in **Table 2** and the data of untreated specimen are quoted from our previous study [12]. AZ91D Mg alloy is composed mainly of α phase (Mg) and β phase ($Mg_{17}Al_{12}$). After 30s HF acid pickling-activation, the specimen surface is smooth and slightly non-uniform dissolved along the interface of β phase and

α phase, where some micro-cracks and pits are found as shown in **Fig. 1A**. In **Table 2**, after HF acid pickling-activation, EDX results show that the quantity of Mg and Al element in β phase is less than that of untreated β phase and oxygen is also detected, especially in the dissolution parts along boundaries between α phase and β phase (Point **a**). Therefore, the HF acid pickling-activation results in the slight dissolution of β phase on the specimen surface and α phase is passivated correspondingly, which decreases the difference of the chemical activity between α phase and β phase. Therefore, one-step HF pickling-activation not only removes the loose film on the magnesium alloy surface, but also avoids fierce replacement which is propitious to plate smooth layers.

Table 2 EDX results of AZ91D Mg alloy after different pretreatment steps (wt %)

Samples	Regions	Mg	Al	Zn	O	Cu
Untreated [12]	α phase	92.12	7.83	_	_	_
	β phase	59.82	35.86	4.32	_	_
After HF acid pickling-activation	α phase	92.45	7.55	_	_	_
	β phase	55.24	32.99	4.74	7.03	_
	Point a	58.19	27.64	6.30	7.87	_
After Zn immersion	α phase	95.71	_	4.29	_	_
	Point b	33.35	_	66.65	_	_
After copper plating	_	_	_	_	_	100

After the process of zinc immersion, the deposited network-Zn layer is formed on the specimen after one-step HF pickling-activation as shown in **Fig. 1B**. No Al element and more Zn element are detected as EDX results shown in **Table 2**, indicating the β phase is gradually dissolved and then coved by Zn layer during the process of Zn immersion. The reduction of Zn occurs preferentially on β phase of the electrode surface in the Zn immersion bath and then the Zn layer will extend to α phase until all the surface of specimen is covered. Therefore the difference between α phase and β phase is reduced, in other words, the chemical activity and Volta electrode potential diversity distribution on the substrate is equalized and potential difference between magnesium alloy substrate and subsequent deposits is reduced after zinc immersion process.

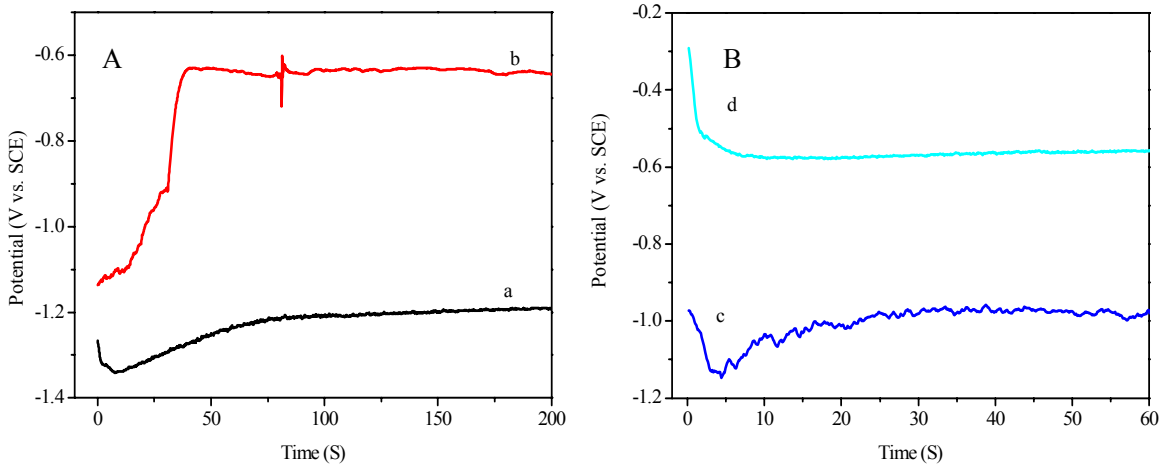

Fig. 2 A. OCPs with time of AZ91D Mg alloy in Cu plating bath after (a) HF acid pickling-activation, and (b) Zn immersion, temperature was controlled at 40℃; B. OCPs with time of AZ91D Mg alloy in Ni-P plating bath after (c) Zn immersion and (d) Cu plated, temperature was controlled at 70℃.

The changes of OCP with time of AZ91D Mg alloy specimen after different pretreatments in Cu plating bath are shown in **Fig. 2A.** The potential of specimen after acid pickling first deceases

from -1.27 V_{SCE} to -1.34 V_{SCE} during the initial 9s, suggesting activation dissolution of the substrate. Then the potential slowly increases to a steady lower potential (-1.21 V_{SCE}) within about 75s, indicating some Cu is deposited on the substrate. However, the OCP of the specimen after Zn immersion immediately ascends to a steady nobler potential stage (-0.63 V_{SCE}) within 40s without decrease, indicating that Zn layer can efficiently prevent the corrosion attack of the plating solution to the substrate. The results of OCP in **Fig. 2A** indicate that the electrode surface covered by Zn layer is more thermodynamically steady than that of the one after HF acid pickling-activation in the Cu plating bath. Therefore the specimen is more difficult to be electroplated than to be dissolved during copper plating without Zn immersion.

Integrated and compact Cu as-deposited layer with a typical nodular surface morphology is shown in **Fig. 1C**. XRD pattern (Fig. ommited.) also shows the sharp peaks corresponding to Cu. Therefore, a Cu layer is electroplated on the AZ91D specimen successfully.

Fig. 2B shows the evolutions of E_{OCP} with time of the specimens after different pretreatments in Ni-P plating bath. The **curve d** descends first and then quickly stay steady potential (-0.57 V_{SCE}) within initial 2.0 s, which indicates the specimen after copper plated has the higher steady potential in the Ni-P plating bath. The specimen after Zn immersion without Cu plated has a lower potential (-1.0 V_{SCE}) as shown in the **curve c** which descends first and then ascends to a fluctuant potential stage, indicating the specimen after Zn immersion without Cu plated is unsteady in Ni-P plating bath. In other words, the AZ91D Mg alloy after once Zn immersion uncoated by Cu layer tends to be seriously corroded in the acid Ni-P plating bath, on which Ni-P coatings can't be electrodeposited successfully. However, the specimen coated by dense Cu layer after Zn immersion can effectively prevent specimen being corroded in the acid Ni-P plating bath in the initial stage, on which Ni-P coatings can be electrodeposited successfully. **Fig. 1D** shows the surface morphology of Ni-P coatings without Cu plated as a protective under-layer. Obviously, the Ni-P coatings is rough, loose and porosity, comparing with the dense and pore-free surface morphology of Ni-P coatings with Cu as a protective under-layer (**Fig. 4**). Ni-P coatings on magnesium alloy function as the cathode coating due to that the standard electrode potential of Ni-P alloy is higher than that of the AZ91D Mg alloy specimen. The Ni-P deposits must be pore-free; otherwise, the corrosion of the substrate will be accelerated. In addition, as the standard electrode potential of Cu is higher than that of Ni-P alloys, the Cu layer can function as a long-term protective layer for Mg alloy substrate during the long-term anodic dissolution of Ni-P coatings.

2.2 Morphologies and Microstructure of Ni-P coatings

The electrodepositing technology parameters, current density (D_k) and the solution pH value, are the main factors to affect the phosphorus content and then the phosphorus content further influence the microstructure, morphology, and anti-corrosion performance of Ni-P coatings. Ni-P coatings with different phosphorous content are obtained by various D_k from 1.0 to 10A/dm^2 and pH value from 0.84 to 2.2. The effect of different phosphorous content on the microstructure and morphology of the Ni-P coatings obtained by various D_k is studied (**Figs. 3** and **4**).

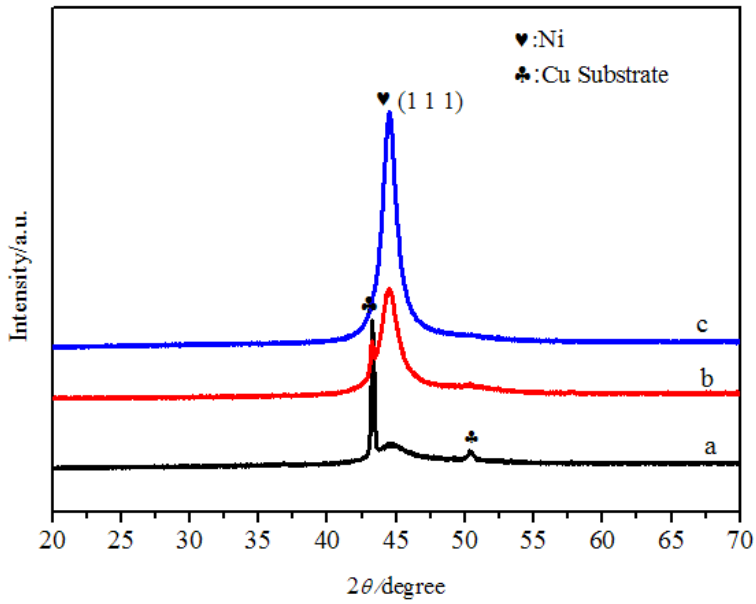

Fig. 3 XRD patterns of the electrodeposited Ni-P coatings with different P content (a) Ni-18.92 at% P, (b) Ni-16.71 at% P and (c) Ni- 7.42 at% P.

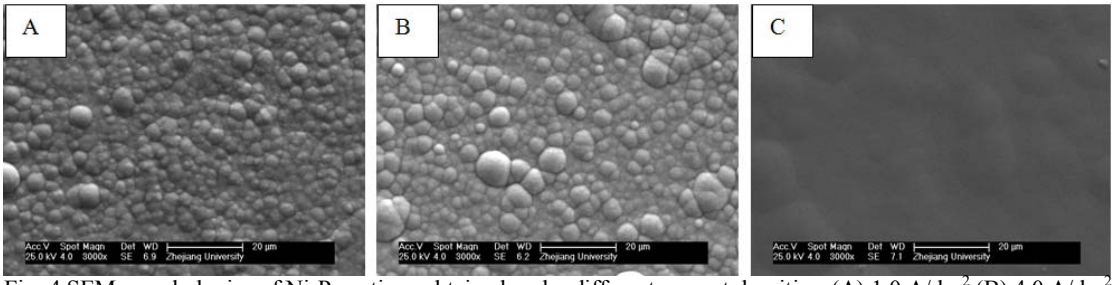

Fig. 4 SEM morphologies of Ni-P coatings obtained under different current densities: (A) 1.0 A/dm^2 (B) 4.0 A/dm^2 (C) 10.0 A/dm^2, pH=2.0.

X-ray diffraction patterns of Ni-P coatings with various phosphorus contents are shown in **Fig. 3**. Besides the peaks of Cu under-layer, there is only a wide diffraction peak corresponding to pure nickel as shown in **curve a**, which means the structure of the Ni-P coatings with 18.92% phosphorus is amorphous. The peaks corresponding to Cu in the Ni-P coatings (**curves a** and **b**) are attributed to that the Ni-P coatings obtained at lower current density are too thin. With the phosphorus contents decreasing to 7.42 at.%, the peaks around 2θ=45° corresponding to the prominent (111) peak of pure nickel become sharp (**curves b** and **c**), indicating the Ni-P gain is gradually coarsening and demonstrating the coatings are amorphous-microcrystalline or microcrystalline structure. These results indicate that coatings are transformed from amorphous phase to microcrystalline structure with a decrease of phosphorus contents, which is in agreement with the results reported earlier [13, 20].

Fig. 4 shows the surface morphologies of Ni-P coatings obtained under various current densities. The surface morphologies exhibit compact and uniform appearance changing from "cauliflower-like" to "mirror-like" gradually with an increase of the current density coupled with a decrease of phosphorus contents (**Fig. 4**). In **Fig. 4A,** the surface morphology appears to be composed of larger nodules of "cauliflower" type structures typical for amorphous materials [21]. As phosphorus content decreases to 7.42 at.% in Ni-P coatings obtained under the current density at 10 A/dm^2 (**Fig. 4c**), the grain size got finer corresponding to microcrystalline structure, in agreement with X-ray diffraction results.

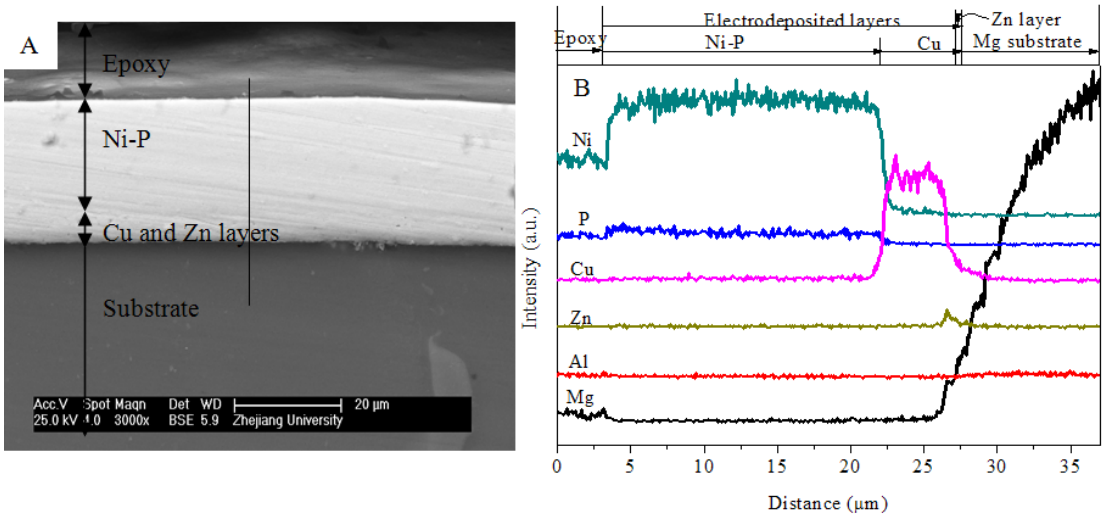

Fig. 5 The cross section morphology (A) and EDX line profile (B) for the Ni-P coatings electrodeposited at D_k=8 A/dm^2, pH=2.0.

Fig. 5 shows the cross section morphology and EDX line profile of the Ni-P alloy coatings. The pretreatments prior to electroplating Cu under-layer for the AZ91D Mg alloy provide the surface pits to act as sites for mechanical interlocking to improve adhesion. The immersion Zn layer is located in the area where the substrate specimen and Cu layer mutually overlap. Though the substrate is not completely covered with a coherent zinc layer (**Fig. 1B**), the deposited Zn layer strengthens the adhesion of the subsequently deposited Cu layer to Mg alloy substrate. There is no obvious boundary or interfacial defects observed along the interface between the Cu under-layer and the Ni-P coatings, indicating Ni-P coating is attached tightly to the Cu under-layer with the typical nodular surface (**Fig. 1C**). In addition, the Ni-P coating is very compact and no pores exist in its cross section morphology (**Fig. 5A**). The elements distribution from the coating surface to the substrate along the line labeled in **Fig. 5B**. Some Ni element which may be brought during the polishing process is detected in the epoxy resin. Form **Fig. 5B**, the Ni-P coatings with a thickness of about 20 μm, a dense Cu layer with a thickness of 6 μm, the Zn layer and the AZ91D Mg alloy substrate are connected closed.

2.3 Corrosion properties of Ni-P coatings

The electrodepositing technological parameters indicate that current density (D_k) and pH values significantly affect the phosphorus content, morphology, structure and anti-corrosion character of Ni-P deposits. The Ni-P coatings are gradually transformed to amorphous structure with increasing the phosphorous content by varying the current density and pH value of Ni-P electrolyte whose optimize ranges are 2.0~8.0 A/dm^2 and 1.0~2.0, respectively. In fact, the Ni-P coatings turned out to be burnt partially at the electrode edge when the solution pH value and the current density (D_k) are higher than 2.3 and 14 A/dm^2, respectively.

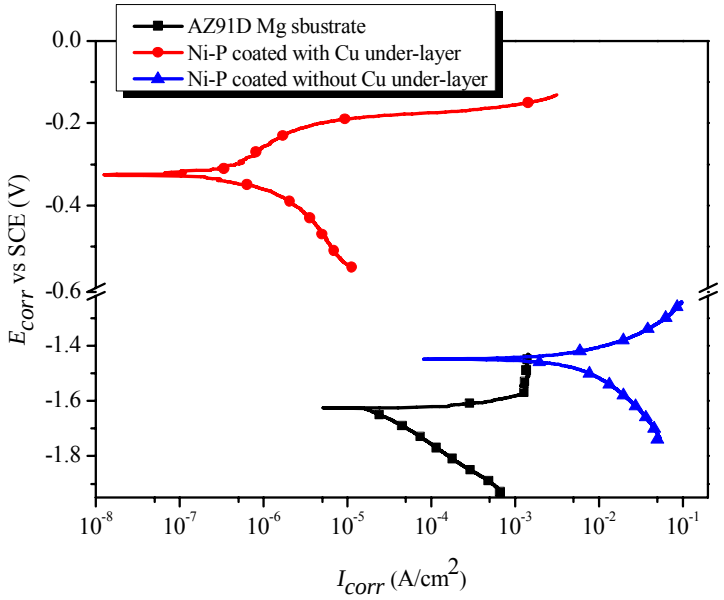

Fig. 6 Polarization curves of substrate and Ni-P coatings in neutral 3.5 wt. % NaCl at room temperature.

The potentiodynamic polarization curves of as-deposited Ni-P coatings obtained at pH=1.6, D_k=8 A/dm^2 with and without plated Cu as a protective under-layer and AZ91D Mg alloy substrate are shown in **Fig. 6**. The parameters fitted from the polarization curves are listed in **Table 3**.

Table 3 The parameters obtained by fitting the Polarization curves of specimens.

Specimens	E_{corr}(V vs SCE)	I_{corr} (μA/cm^2)	b_c (mV/dec)
AZ91D substrate	-1.62	30.67	200
Ni-P with plated Cu	-0.32	0.30	95
Ni-P without plated Cu	-1.45	6758	230

From **Table 3**, the corrosion potential of Ni-P coatings with Cu under-layer is about 1.3 V higher than the AZ91D Mg alloy substrate, indicating that the former is a more thermodynamically steady system. Meanwhile, the corrosion current density of the Mg alloy substrate is about two orders of magnitude higher than that of Ni-P coatings, indicating the Ni-P coatings improve the anti-corrosion performance of AZ91D Mg alloy markedly. Therefore, an electrodeposited Ni-P coating is an ideal corrosion protective layer for AZ91D Mg alloy. The slope of cathodic curve (b_c value) of Ni-P coated decreases to 95 mV/dec from 200 mV/dec of Mg alloy substrate without Ni-P deposit, indicating that Ni-P coatings can accelerate the hydrogen evolution [15]. There are great changes of the corrosion potential and corrosion current density between Ni-P coatings with and without plated Cu as a protective under-layer. The Ni-P coatings with plated Cu shows a higher corrosion potential (E_{corr}= -0.32 V_{SCE}) and a lower corrosion current density (I_{corr}=0.30 μA/cm^2) than the one without plated Cu. Therefore, the Ni-P deposit without plated Cu has no protective ability for AZ91D Mg alloy, owning to its rough and defective surface (**Fig. 1D**) and the fragmentary Ni-P coatings as cathode part prone to galvanic corrosion with Mg alloy substrate in neutral 3.5 wt. % NaCl solution.

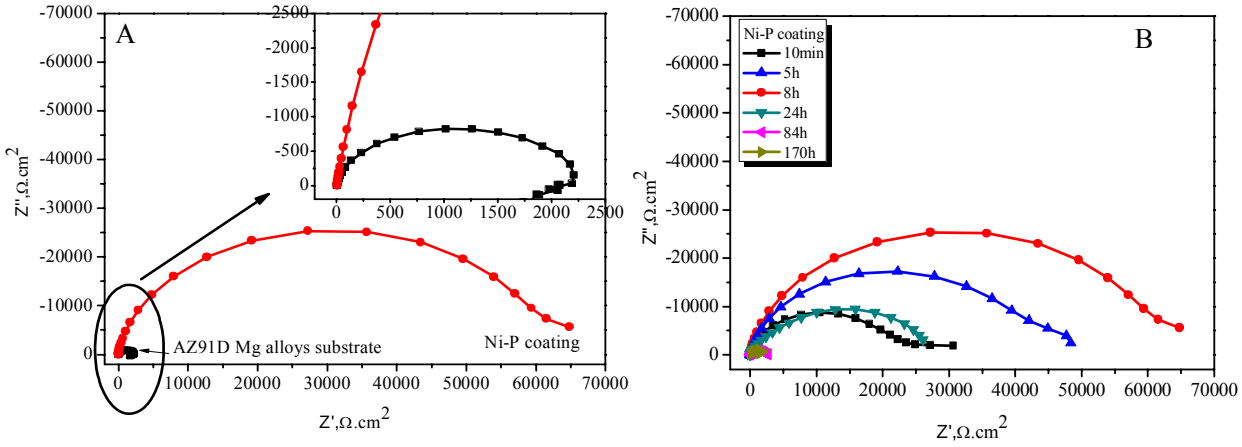

Fig. 7 Nyquist plots of (A) the coated Ni-P alloys and the AZ91D Mg alloy substrate without coated Ni-P alloys immersion for 10 min, (B) long-term immersion of Ni-P coatings in neutral 3.5 wt. % NaCl solution at room temperature.

The anticorrosion performance of Ni-P coatings is also investigated by the EIS. Typical Nyquist plots of the coated Ni-P alloys and AZ91D Mg alloy substrate without coated Ni-P alloys immersion for 10 min (**A**) and Ni-P coatings obtained at pH=2.0, D_k=8 A/dm^2 for long-term immersion (**B**) in neutral 3.5 wt.% NaCl solution at room temperature are presented in **Fig. 7**. Generally, these Nyquist diagrams of Ni-P coatings show a semi-elliptic arc in the investigated frequency range, while, the one of the Mg alloy substrate exists a low-frequency inductive loop which may be originated from the pitting corrosion on the Mg alloy electrode surface [24]. In addition, the axial radius of the semi-elliptic arc of Ni-P coatings is larger than that of the Mg alloy substrate, which indicates that the polarization resistance of the Ni-P coatings is markedly higher than that of the uncoated AZ91D Mg alloy. In other word, the anticorrosion ability of AZ91D Mg alloy substrate is greatly improved by the Ni-P coatings, which is in agreement with the results of potentiodynamic polarization behavior of the AZ91D Mg alloy with and without Ni-P coated (**Fig. 6**). The high polarization resistance benefits from the dense and pore-free amorphous or microcrystalline structure of Ni-P coatings, which availably obstructs the attack of Cl^- in NaCl solution.

The EIS of Ni-P coatings in NaCl solution for long-term immersion are shown in **Fig. 7B**. With the long-term immersion time, the axial radius of the semi-elliptic arc increases to the maximum after 8 hours immersion and then decreases, indicating the polarization resistance of the Ni-P coatings first increases and then decreases during the long-term immersion in NaCl solution. In general, the polarization resistance of the Ni-P coatings decreases during the long-term immersion as the attack of Cl^- [25]. However, the polarization resistance of Ni-P coatings shows a maximum value after 8 hours immersion in this work, It may be ascribed to the dissolution of the nickel atom on Ni-P coatings surface during the long-term immersion in the NaCl media, resulting in gradual accumulation of the phosphorus content and thus the Ni-P coatings is passivation in the initial immersion stage. Meanwhile, as the standard electrode potential of the Cu is higher than that of Ni-P alloys, the Cu plated under-layer can function as a cathodic protective layer, assisting Ni-P coatings in obstructing the attack of Cl^- during the anodic dissolution of Ni-P coatings in the initial immersion stage. Therefore, the polarization resistance of Ni-P coatings in long-term immersion in NaCl solution exist a maximum value in the initial stage.

3 Conclusion

The Cu coating as a protective under-layer is electrodeposited on AZ91D Mg alloy after one step HF acid pickling-activation and once Zn immersion and the nodular surface is of good adherence to the substrate and the further Ni-P coatings. The optimize ranges of the technology parameters of the pH value and the current density for Ni-P electrodeposition are 2~8 A/dm^2 and 1.0~2.0, respectively. High corrosion resistance Ni-P coatings with the phosphorus content from 8.8 to 17.0 at.% are obtained. With increasing the phosphorous content of the Ni-P coatings, the structure is gradually transformed to amorphous and the corrosion resistance increases synchronously. The potentiodynamic polarization curves show that the corrosion current density of the AZ91D Mg alloy coated by Ni-P coatings is about two orders of magnitude less than that of the uncoated one and EIS shows that the polarization resistance of the Ni-P coatings is larger than that of the AZ91D Mg alloy substrate. Cu plated under-layer functions as a cathodic protective layer, assisting Ni-P coatings in obstructing the attack of Cl^- during the anodic dissolution of Ni-P coatings in the initial immersion stage in NaCl solution.

References

[1] Gray J E, Luan B. Protective coatings on magnesium and its alloys -- a critical review(J). Journal of Alloys and Compounds, 2002, 336:88-113.
[2] Gu C, Lian J, Li G, Niu L, Jiang Z. Electroless Ni-P plating on AZ91D magnesium alloy from a sulfate solution(J). Journal of Alloys and Compounds, 2005, 391:104-109.
[3] Jiang Y F, Zhai C Q, Liu L F, Zhu Y P, Ding W J. Zn-Ni alloy coatings pulse-plated on magnesium alloy(J). Surface and Coatings Technology, 2005, 191:393-399.
[4] Huang C A, Wang T H, Weirich T, Neubert V. Electrodeposition of a protective copper/nickel deposit on the magnesium alloy (AZ31)(J). Corros Sci, 2008, 50:1385-1390.
[5] Chong K Z, Shih T S. Conversion-coating treatment for magnesium alloys by a permanganate-phosphate solution(J). Materials Chemistry and Physics, 2003, 80:191-200.
[6] Chang L, Cao F, Cai J, Liu W, Zhang J, Cao C. Formation and transformation of Mg(OH)2 in anodic coating using FTIR mapping(J). Electrochemistry Communications, 2009, 11:2245-2248.
[7] Cai J, Cao F, Chang L, Zheng J, Zhang J, Cao C. The preparation and corrosion behaviors of MAO coating on AZ91D with rare earth conversion precursor film(J). Appl Surf Sci, 2011, 257:3804-3811.
[8] Lamaka S V, Montemor M F, Galio A F, Zheludkevich M L, Trindade C, Dick L F, Ferreira M G S. Novel hybrid sol-gel coatings for corrosion protection of AZ31B magnesium alloy(J). Electrochim Acta, 2008, 53:4773-4783.
[9] Nordlien J H, Ono S, Masuko N, Nisancioglu K. A TEM investigation of naturally formed oxide films on pure magnesium(J). Corros Sci, 1997, 39:1397-1414.
[10] Huang C A, Lin C K, Yeh Y H. Increasing the wear and corrosion resistance of magnesium alloy (AZ91D) with electrodeposition from eco-friendly copper- and trivalent chromium-plating baths(J). Surface and Coatings Technology, 2010, 205:139-145.
[11] Huang C A, Wang T H, Weirich T, Neubert V. A pretreatment with galvanostatic etching for copper electrodeposition on pure magnesium and magnesium alloys in an alkaline copper-sulfate bath(J). Electrochim Acta, 2008, 53:7235-7241.
[12] Zhao M J, Cai C, Wang L, Zhang Z, Zhang J Q. Effect of zinc immersion pretreatment on the electro-deposition of Ni onto AZ91D magnesium alloy(J). Surface and Coatings Technology, 2010, 205:2160-2166.
[13] Hu C C, Bai A. Influences of the phosphorus content on physicochemical properties of nickel-phosphorus deposits(J). Materials Chemistry and Physics, 2003, 77:215-225.
[14] Bai A, Chuang P-Y, Hu C-C. The corrosion behavior of Ni-P deposits with high phosphorous contents in brine media(J). Materials Chemistry and Physics, 2003, 82:93-100.
[15] Petukhov I V, Shcherban M G, Skryabina N E, Malinina L N. Corrosion and Electrochemical Behavior of Ni-P Coatings in 0.5 M H2SO4(J). Protection of Metals, 2002, 38:370-376.
[16] Wu L P, Zhao J J, Xie Y P, Yang Z D. Progress of electroplating and electroless plating on magnesium alloy(J). T Nonferr Metal Soc, 2010, 20:s630-s637.
[17] Brenner A, Couch D E, Williams E K. J. The composition of the bath is CoCO3 (39.4 g/l-0.33M), CoCl3o6H2O (181 g/l-0.76M), H3PO3 (65 g/l-0.76M), and H3PO4 (50 g/l-0.51M) (J). Electrodeposition temperature: 80 C. Res. Natl. Bur. Stand., 1950, 44:109-114.
[18] Zeller R L, Iii, Landau U. Electrodeposition of Ni-P Amorphous Alloys(J). J. Electrochem. Soc., 1992, 139:3464-3469.
[19] Zhu Y, Yu G, Hu B, Lei X, Yi H, Zhang J. Electrochemical behaviors of the magnesium alloy substrates in

various pretreatment solutions(J). Appl Surf Sci, 2010, 256:2988-2994.
[20] Yuan X, Sun D, Yu H, Meng H. Structure and mechanical properties of Ni-P electrodeposited coatings(J). Appl Surf Sci, 2009, 255:3613-3617.
[21] Mahalingam T, Raja M, Thanikaikarasan S, Sanjeeviraja C, Velumani S, Moon H, Kim Y D. Electrochemical deposition and characterization of Ni-P alloy thin films(J). Mater Charact, 2007, 58:800-804.
[22] Saitou M, Okudaira Y, Oshikawa W. Amorphous structures and kinetics of phosphorous incorporation in electrodeposited Ni-P thin films(J). J. Electrochem. Soc., 2003, 150:C140-C143.
[23] Ma C B, Cao F H, Zhang Z, Zhang J Q. Electrodeposition of amorphous Ni-P coatings onto Nd-Fe-B permanent magnet substrates(J). Appl Surf Sci, 2006, 253:2251-2256.
[24] Metikoš-Huković M, Babić R, Grubač Z, Brinć S. Impedance spectroscopic study of aluminium and Al-alloys in acid solution: inhibitory action of nitrogen containing compounds(J). Journal of Applied Electrochemistry, 1994, 24:772-778.
[25] Wang L L, Chen H J, Huang W Q. Electrochemical corrosion behavior of electroless Ni–P coating in NaCl and H2SO4 solutions(J). Materials and Corrosion, 2010, DOI: 10.1002/maco.200905575

AZ91D 镁合金电沉积保护性 Cu/Ni-P 镀层

张珊，曹发和，郑俊军，张昭，张鉴清
（浙江大学化学系，杭州 310027）

摘要：通过优化的前处理，包括一步酸洗活化和一次侵锌，在 AZ91D 镁合金表面电沉积制备了高耐蚀的 Cu/Ni-P 镀层。考察了 pH 值和电流密度等对 Ni-P 镀层 P 含量及其耐蚀性能的影响，结果表明随着 Ni-P 镀层 P 含量的降低，镀层从微晶态转变为非晶态，耐蚀性能提高。电化学测试结果表明 Cu 沉积层有利于在镁合金表面 Ni-P 电沉积，自腐蚀电流密度较 AZ91D 镁合金减低 2 个数量级以上。

关键词：AZ91D 镁合金；电沉积；Ni-P；耐蚀性能
中图分类号：TG174.4